



Heriot-Watt University  
Research Gateway

## Simulation of carbonated water injection coreflood experiments

### Citation for published version:

Foroozesh, J & Jamiolahmady, M 2016, 'Simulation of carbonated water injection coreflood experiments: An insight into the wettability effect', *Fuel*, vol. 184, pp. 581-589. <https://doi.org/10.1016/j.fuel.2016.07.051>

### Digital Object Identifier (DOI):

[10.1016/j.fuel.2016.07.051](https://doi.org/10.1016/j.fuel.2016.07.051)

### Link:

[Link to publication record in Heriot-Watt Research Portal](#)

### Document Version:

Peer reviewed version

### Published In:

Fuel

### General rights

Copyright for the publications made accessible via Heriot-Watt Research Portal is retained by the author(s) and / or other copyright owners and it is a condition of accessing these publications that users recognise and abide by the legal requirements associated with these rights.

### Take down policy

Heriot-Watt University has made every reasonable effort to ensure that the content in Heriot-Watt Research Portal complies with UK legislation. If you believe that the public display of this file breaches copyright please contact [open.access@hw.ac.uk](mailto:open.access@hw.ac.uk) providing details, and we will remove access to the work immediately and investigate your claim.

Manuscript Number: JFUE-D-16-01367R1

Title: Simulation of Carbonated Water Injection Coreflood Experiments: An Insight into the Wettability Effect

Article Type: Research paper

Keywords: Carbonated water injection (CWI); Mass transfer kinetics; Coreflood Experiments; Oil swelling; Wettability

Corresponding Author: Dr. Jalal Foroozesh, Ph.D.

Corresponding Author's Institution: Heriot-Watt University

First Author: Jalal Foroozesh, Ph.D.

Order of Authors: Jalal Foroozesh, Ph.D.; Mahmoud Jamiolahmady, Ph.D.

Abstract: In this paper, our previously developed model (simulator) has been used to simulate and study a different CWI coreflood experiment from the literature performed in a mixed-wet sandstone core. The developed model which was based on mass transfer kinetics had been used before to simulate a coreflood experiment performed in a water-wet sandstone rock. In this paper, a different procedure has been applied for the simulation of CWI in the mixed-wet core. That is, in contrast to the water-wet coreflood test where only mass transfer parameter was tuned, here, both mass transfer parameter and relative permeability curves have been obtained through a history matching experiment applying our genetic algorithm (GA) based optimization program. Furthermore, using the simulation results, it has been observed that in addition to oil swelling and contrary to the water-wet core, wettability alteration is also an important recovery mechanism for the mixed-wet core. The potential of CO<sub>2</sub> storage during the mixed-wet CWI coreflood experiment has also been investigated. The results obtained in this paper can help to crosscheck and verify the performance of the developed simulator and also to explore its generic capability. Moreover, the results of this paper gives an insight into different recovery mechanisms contributing during CWI coreflood experiments.

- A CWI coreflood experiment performed in a mixed-wet core is studied mathematically.
- Compared to CWI in a water-wet core, a different simulation procedure is suggested.
- The contribution of both wettability alteration and oil swilling mechanisms is discussed.



26 **Keywords:** Carbonated water injection (CWI); Mass transfer kinetics; Coreflood  
27 Experiments; Oil swelling; Wettability

## 28 **1. Introduction**

29 Carbonated water (CW) injection is a CO<sub>2</sub>-EOR method where CO<sub>2</sub> is used efficiently. In  
30 carbonated water injection (CWI) technique and compared to conventional water injection  
31 (WI), water will be saturated with CO<sub>2</sub> before injecting into oil reservoirs. Upon contact of  
32 CW with oil in the reservoir, CO<sub>2</sub> starts migrating to the oil phase due to its higher solubility  
33 in hydrocarbons compared to water, which results in a higher oil recovery factor. During  
34 CWI, CO<sub>2</sub> stays dissolved in oil and water phases and not as a free phase, therefore it gives a  
35 better sweep efficiency compared to the pure CO<sub>2</sub> injection strategy. Moreover, contrary to  
36 the pure CO<sub>2</sub> injection strategy, CWI needs less amount of CO<sub>2</sub> making it an attractive CO<sub>2</sub>-  
37 EOR strategy for offshore fields, where the supply of CO<sub>2</sub> is limited. Furthermore, through  
38 CWI and at the end of the injection period, some amount of CO<sub>2</sub> (as a greenhouse gas) is  
39 stored in the reservoir securely as is dissolved in remaining oil and water [1-4]. CWI has been  
40 investigated experimentally and mathematically in the literature. Experimental study of CWI  
41 has mainly been focused on flooding tests including cores [4-9] and sand packed set-ups [10,  
42 11]. Direct visualization of flow during CWI using high-pressure transparent micro-model  
43 set-up (high pressure Hele-Shaw) has also been considered in the literature [4, 12, 13]. All the  
44 reported experiments show an increased recovery factor obtained by CW over conventional  
45 WI with some CO<sub>2</sub> stored in the system at end of the experiments. The experiments could  
46 help to understand the mechanisms involved during CWI. When CO<sub>2</sub> migrates to the oil  
47 phase during CWI, it increases the oil volume (oil swelling) and decrease its viscosity, and  
48 reduces IFT of water-oil system all resulting in a better recovery factor [4, 5, 12-14].  
49 However the wettability of rock also affect the efficiency of CWI process. Sohrabi et al. [5]  
50 performed a series of CWI coreflood experiments in a water-wet and a mixed-wet aged core.

51 They observed that under the same conditions, the recovery obtained for the aged core was  
52 higher. The change of wettability of the rock in the presence of CO<sub>2</sub> and specifically by  
53 carbonated water is reported in the literature. Yang et al.[15] experimentally measured the  
54 contact angle of a crude oil-carbonate rock –carbonated brine system at high pressure and  
55 temperatures. A change in contact angle (around 20°) from oil-wet towards intermediate-wet  
56 (neutral-wet) due to the presence of CO<sub>2</sub> in the system was observed quickly (in less than 10  
57 minutes). Seyyedi et al.[16] performed a series of contact angle measurements to determine the  
58 wettability of three different minerals (substrates) of quartz (the main mineral of sandstone  
59 rocks), mica, and calcite (the main mineral of carbonate rocks) in the presence of a crude oil and  
60 carbonated brine at reservoir conditions. In addition to clean substrates, the substrates were also  
61 aged in the same crude oil to measure the contact angle of aged minerals as well. The aged quartz  
62 showed a contact angle change from 76° to 61° (natural-wet towards water-wet) and for the aged  
63 calcite a contact angle change from 144° to 97° was observed (oil-wet towards neutral-wet) due to  
64 CO<sub>2</sub> dissolution in brine. For the unaged minerals, a small change in contact angle was observed  
65 (around 5° or less). To provide more support to the idea of wettability change during CWI,  
66 Seyyedi and Sohrabi [17] performed a series of spontaneous imbibition tests at reservoir  
67 conditions using aged and unaged sandstone and carbonate rock samples. No spontaneous  
68 imbibition was observed for aged sandstone and carbonate samples when brine was used whereas  
69 carbonated water could imbibe into the rock sample. Al-Mutairi et al.[18] measured the  
70 wettability of an aged carbonate rock sample under 500 psi pressure and 70 °C. They  
71 observed that the contact angle was changed quickly (in less than one hour) from 101° to 83°  
72 when it was contacted by carbonated water. Wettability alteration by carbonated water has also  
73 been observed in micro-model set-up. Based on some observation in a micro-model set-up,  
74 Sohrabi et al.[5] realized that the shape of oil ganglia trapped were more rounded after CWI  
75 compared to those after WI. They expressed that this difference in shape of oil blobs indicates  
76 that the surface of micro-model has become more water-wet after CWI. All these studies show

77 that the carbonated water can change the wettability of rock surfaces specifically the oil-wet  
78 surfaces to neutral-wet surfaces or neutral-wet surfaces to more water-wet surfaces, but it has a  
79 minimal effect on water-wet or strong water-wet surfaces. As compared to experimental study,  
80 mathematical modeling and simulation of CWI process has not been studied much in the  
81 literature. De Nevers[19] presented an analytical model based on the Buckley–Leveret  
82 theory to predict the CWI performance. Ramesh and Dixon [20] presented a numerical black-  
83 oil based model to predict the performance of Carbone Dioxide (CO<sub>2</sub>) flooding and CWI into  
84 heterogeneous oil reservoirs. Chang et al.[21] developed a three-dimensional, three-phase  
85 compositional simulator to include the impact of CO<sub>2</sub> solubility in water during CO<sub>2</sub>  
86 injection. In the compositional model mentioned above, the assumption of instantaneous  
87 equilibrium was applied. This assumption implies that in a simulation grid block, distribution  
88 of CO<sub>2</sub> between water and oil happens instantly to reach an immediate equilibrium state.  
89 Kechut et al.[6] used ECLIPSE300 (E300) commercial software to simulate some available  
90 CWI coreflood experiments. They argued that E300 can not properly simulate this process  
91 due to intrinsic assumption of instantaneous equilibrium made by E300 which is not valid for  
92 CWI coreflood experiments. As mentioned in the literature[22], this assumption can lead to  
93 large errors where for example there are short contact times for mass transfer process  
94 (laboratory displacement in cores) or large diffusion patterns are available for components to  
95 diffuse through them (field scale) and moreover, if there is slow diffusion velocities due to  
96 large viscosity of resident fluids. Accordingly, we previously developed a new compositional  
97 simulator (model) for simulating CWI process based on mass transfer kinetics where the  
98 assumption of instantaneous equilibrium was relaxed[1]. We used the developed model for  
99 simulation of a CWI coreflood experiment carried on in an unaged water-wet core. In this  
100 article we will use the developed model for simulation of a different CWI coreflood  
101 experiment from the literature carried on in an aged mixed-wet core. The simulation results

102 are interpreted to discover different recovery mechanisms of CWI in water-wet and mixed-  
 103 wet cores. That is, the main goal here is to explore the role of rock wettability and wettability  
 104 alteration in the performance of CWI process by considering the experimental data of two  
 105 cores with different wettabilities. The structure of this paper is: first, a summary of the  
 106 developed model is presented, next, the results of coreflood experiments are presented and  
 107 discussed, later the details of simulations and the interpretations of the results are expressed  
 108 in detail.

## 109 2. Mathematical model

110 A summary of model developed in our previous paper[1] is presented here. The model is  
 111 one-dimensional, two-phase (oil and water) developed for a system having three components  
 112 (oil, water and CO<sub>2</sub>). The oil phase is a mixture of oil and CO<sub>2</sub> components and the water  
 113 phase is a mixture of water and CO<sub>2</sub> components. It should be mentioned that during CWI,  
 114 there is no free CO<sub>2</sub> in the system as all the present CO<sub>2</sub> are dissolved in oil and water phases.  
 115 The assumptions of no chemical reaction, no gravity effect and having dead oil without any  
 116 liberated gas in the system are applied. The dead oil is considered as a single pseudo  
 117 component. The PDE governing equations are continuity equations of each component in the  
 118 system as given below:

$$\varphi \frac{\partial(\rho s \omega)}{\partial t} = - \frac{\partial(\rho u \omega)}{\partial x} \quad (1a)$$

$$\varphi \frac{\partial(\rho s \omega^{CO_2})}{\partial t} = - \frac{\partial(\rho u \omega^{CO_2})}{\partial x} + U \quad (1b)$$

$$\varphi \frac{\partial(\rho_w s_w \omega_w^w)}{\partial t} = - \frac{\partial(\rho_w u_w \omega_w^w)}{\partial x} \quad (2a)$$

$$\varphi \frac{\partial(\rho_w s_w \omega_w^{CO_2})}{\partial t} = - \frac{\partial(\rho_w u_w \omega_w^{CO_2})}{\partial x} - U \quad (2b)$$

119 Eq. (1a) is the continuity equation of the oil component in the oil phase, Eq. (1b) is the  
 120 continuity equation of the CO<sub>2</sub> component in the oil phase, Eq. (2a) is the continuity equation



121 of the water component in the water phase and Eq. (2b) is the continuity equation of CO<sub>2</sub>  
122 component in the water phase. In the above equations,  $\omega$  and  $\omega^{CO_2}$  are the mass fraction of  
123 oil and CO<sub>2</sub> components in the oil phase, respectively.  $\omega_w^w$  and  $\omega_w^{CO_2}$  are the mass fraction of  
124 water and CO<sub>2</sub> components in the water phase respectively.  $s$  and  $s_w$  are the saturation of  
125 the oil and water phases, respectively. The summation of the mass fraction of components in  
126 each phase and the summation of saturations of oil and water phases are equal to one as a  
127 constraint to the above equations.  $\rho_o$  and  $\rho_w$  are the density (g/cm<sup>3</sup>) of the oil and water  
128 phases, respectively.  $u = -\frac{kKr_o}{\mu_o} \frac{\partial p_o}{\partial x}$  and  $u_w = -\frac{kKr_w}{w} \frac{\partial p_w}{\partial x}$  are the Darcy velocity of the  
129 oil and water phases, respectively.  $p$  and  $p_w$  are the oil and water phase pressures which are  
130 related through the capillary pressure function ( $p_c$ ), i.e.,  $p_c = p - p_w$ .  $Kr$  and  $Kr_w$  are the  
131 relative permeability of oil and water phases, respectively. The Corey correlations shown  
132 below are used to define the relative permeability curves [1, 23]:

$$Kr_w = k_{wmax} s^{*n_w}, \quad Kr_o = k_{omax} (1-s^*)^{n_o}, \quad s^* = \frac{(s_w - s_{wc})}{(1 - s_{wc} - s_{or})} \quad (3)$$

133 The parameters of  $k_{wmax}$ ,  $n_w$ ,  $k_{max}$ ,  $n_o$ ,  $s_{or}$  and  $s_{wc}$  will be obtained through a history  
134 matching experiment. The 'U' (g/cm<sup>3</sup>/sec) added on the right hand side of Eqs. (1b) and  
135 (2b), expresses the value of the CO<sub>2</sub> mass being transferred from the water into the oil phase  
136 as defined below:

$$U = K \times (\rho_w \times \omega_w^{CO_2} \times k_{eq} - \rho_o \times \omega_o^{CO_2}) = K \times (k_{eq} C_w^{CO_2} - C_o^{CO_2}) \quad (4)$$

137 where,  $K = (k_m \times a)$  with 'k<sub>m</sub>' is the overall mass transfer coefficient (cm/sec) and 'a' is the  
138 specific interfacial area (1/cm), which is the oil-water interfacial area per unit volume [24].  $K$   
139 (1/sec) which is a pseudo mass transfer coefficient referred as to MTC parameter here.  $C_w^{CO_2}$   
140 and  $C_o^{CO_2}$  are the CO<sub>2</sub> concentration (g/cm<sup>3</sup>) in oil and water phases.  $k_{eq}$  is the partition  
141 coefficient which is defined as  $k_{eq} = \frac{C_o^{CO_2*}}{C_w^{CO_2*}}$  where  $C_o^{CO_2*}$  and  $C_w^{CO_2*}$  are the CO<sub>2</sub> concentration  
142 (g/cm<sup>3</sup>) in oil and water phases at the equilibrium state. Eq. 4 shows that the rate of CO<sub>2</sub>

143 being transferred is reflected in the MTC parameter and it continues until the CO<sub>2</sub>  
 144 concentration in the water and oil phases reach equilibrium, i.e. become equal to C<sup>CO<sub>2</sub>\*</sup> and  
 145 C<sub>w</sub><sup>CO<sub>2</sub>\*</sup>. The fully implicit finite difference numerical method is used to solve the above PDE  
 146 equations. The details of the solution technique are given in our previous paper[1].

### 147 3. Coreflood Experiments

148 In our previous paper, a set of WI and CWI coreflood experiment performed in a water-  
 149 wet (WW) sandstone core was selected from the literature. In this article, a similar set of WI  
 150 and CWI coreflood experiment but performed in an aged mixed-wet(MW)sandstone core was  
 151 selected from the same literature[5] to be investigated. The experimental conditions of the  
 152 both experiments i.e., water-wet and mixed-wet, were the same (2000 psi and 38 °C). The  
 153 basic core properties used during the experiments are given in Table 1a. Both of the cores had  
 154 been fully saturated by n-decane (n-C<sub>10</sub>H<sub>22</sub>) at 2000 psi and 38 °C. However, in the case of  
 155 the mixed-wet core, the same naturally water-wet sandstone core had been aged using a crude  
 156 oil sample. The fluid properties are given in Table 1b.

157 Table 1a: Basic properties of the water-wet and mixed-wet cores used during the  
 158 experimnts[5].

Core	Length (cm)	Diameter (cm)	Porosity (fraction)	Pore Volume(cm <sup>3</sup> )	Permeability (mD)
Sandstone - WW	33.2	4.986	0.19	123.16	1300
Sandstone - MW	61.3	4.86	0.16	182	850

159  
 160  
 161  
 162

Table 1b: Fluid properties [1].

Fluid	Viscosity(cP) (Test conditions) (136.1 atm, 38 °C)	Density (g/cm <sup>3</sup> ) (Test conditions) (136.1 atm, 38 °C)	Density (g/cm <sup>3</sup> ) Standard conditions (1 atm, 20 °C)
Decane	0.83	0.730	0.727
Water	0.66	0.995	0.995
CO <sub>2</sub>	0.067	0.775	0.00184

163  
 164

165

166

167 It was mentioned that [5] the initial water saturation ( $s_{wi}$ ) had not been established to  
 168 eliminate any influence it may have on the process. However, we think that the initial water  
 169 saturation has minimal effect on the CWI performance. This is because the connate water and  
 170 injected CW would make a single aqueous phase and therefore its presence would have a  
 171 minimal effect on the mass transfer and CO<sub>2</sub> distribution between phases. However, if pure  
 172 CO<sub>2</sub> was injected, the initial water saturation could make a resistant layer for the transfer of  
 173 CO<sub>2</sub> between gas and oil phases. The operational conditions of both experiments are the same  
 174 given in Table 1c. During the both WI and CWI tests, water or carbonated water (CW) was  
 175 injected into the core at a constant rate and water and/or decane were collected at a constant  
 176 pressure at the core outlet. The measured CO<sub>2</sub> content of carbonated water at experimental  
 177 conditions was 5% (weight percent). Recovery factor (RF) or total oil production (TOP) and  
 178 differential pressure (DP) across the core versus the injected pore volume (PV) had been  
 179 recorded during each experiment.

180 Table 1c: The operational conditions of the coreflood experiments[1].

Injection rate (cm <sup>3</sup> /hr)	20
CO <sub>2</sub> mass fraction in injected CW	5 %
Salinity of injected CW (ppm)	10000
Outlet pressure (atm)	136.1
Initial pressure (atm)	136.1
Initial water saturation	0
Temperature (°C)	38

181

182 It is worth mentioning that capillary number ( $N_c = \frac{u_{df} \mu_{df}}{\sigma}$ ) for the experiment was calculated  
 183 to be around 9.8 E-8, which is in the range of typical values of capillary number seen in the  
 184 real oil reservoirs.

185 Figs. 1a and 1b show RF data of the WI and CWI experiments in the WW and MW cores,  
 186 respectively plotted versus injected pore volume (PV). Comparing Figs. 1a and 1b, it can be  
 187 observed that during CWI, oil recovery has improved in both the WW and MW cores. In the  
 188 WW core, WI and CWI have the same breakthrough point with 64% RF and the final RF of  
 189 the CWI after 4.1 PV injected is 73% (equivalent to 90 cm<sup>3</sup> oil production) whereas it is 69%  
 190 (equivalent to 85 cm<sup>3</sup> oil production) for the WI (i.e., 4% additional oil recovery by CWI).  
 191 That is, 9% additional RF after breakthrough has been obtained by CWI. In the MW core,  
 192 however, Fig. 1b shows that CWI and WI have different breakthrough points. The final RF  
 193 of the CWI after 3.3 PV injected is 68% (equivalent to 123.4 cm<sup>3</sup> oil production) while it is  
 194 59% (equivalent to 107.7 cm<sup>3</sup> oil production) for the WI (i.e. 9% additional oil recovery by  
 195 CWI). Moreover, in the MW core, CWI has resulted in 4% additional RF after breakthrough  
 196 point. It can be concluded that CWI has better performance in the aged MW core. Figs. 2a  
 197 and 2b compare DP data of the WI and CWI experiments in the WW and MW cores,  
 198 respectively. Fig. 2a shows that in the WW core, DP data are the same for both the CWI and  
 199 WI experiments. However, in the MW core, CWI has lower DP in comparison with WI  
 200 showing an injectivity improvement during CWI (Fig. 2b).

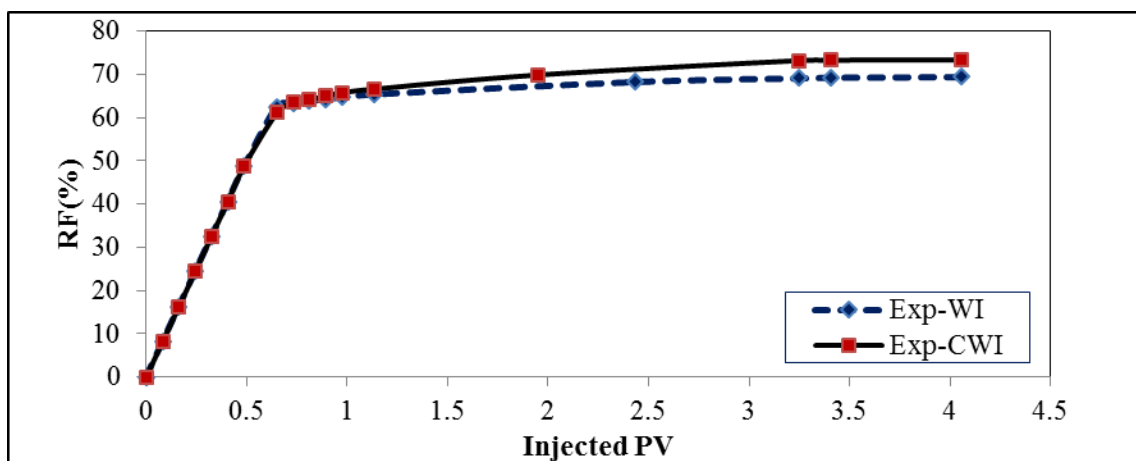


Fig. 1a: Comparison of RF of the WI and CWI experiments, WW core [5].

201  
 202  
 203

204  
205

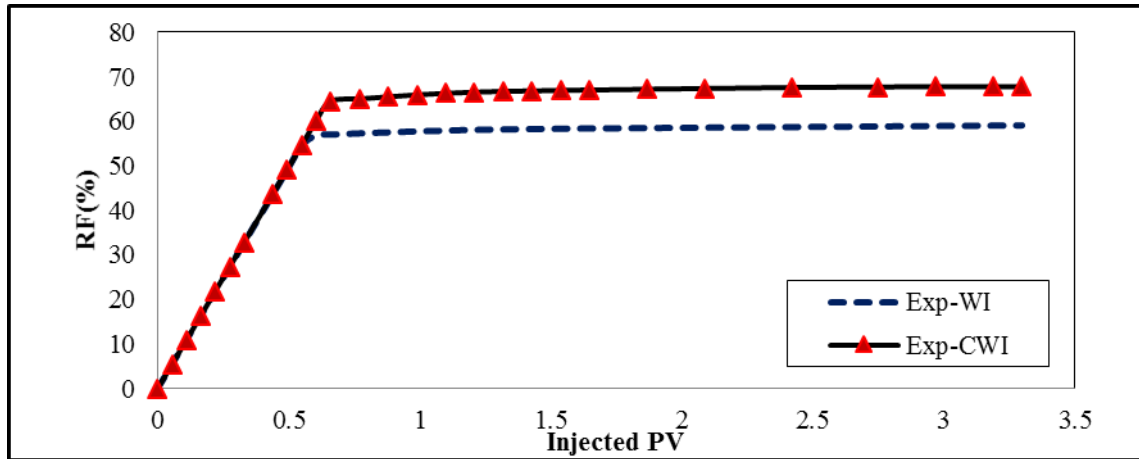


Fig. 1b: Comparison of RF of the WI and CWI experiments, MW core [5].

206  
207

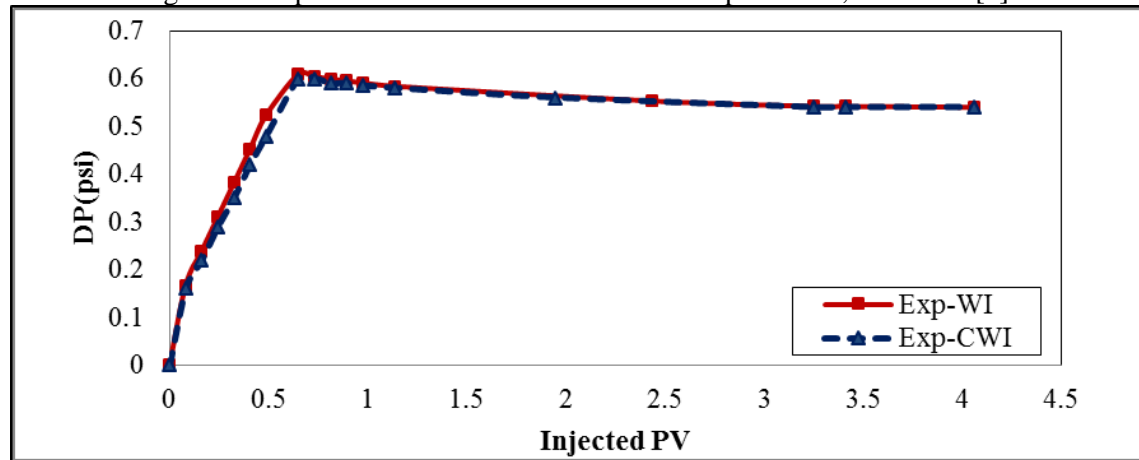


Fig. 2a: Comparison of DP data of the WI and CWI experiments, WW core [5].

208  
209  
210

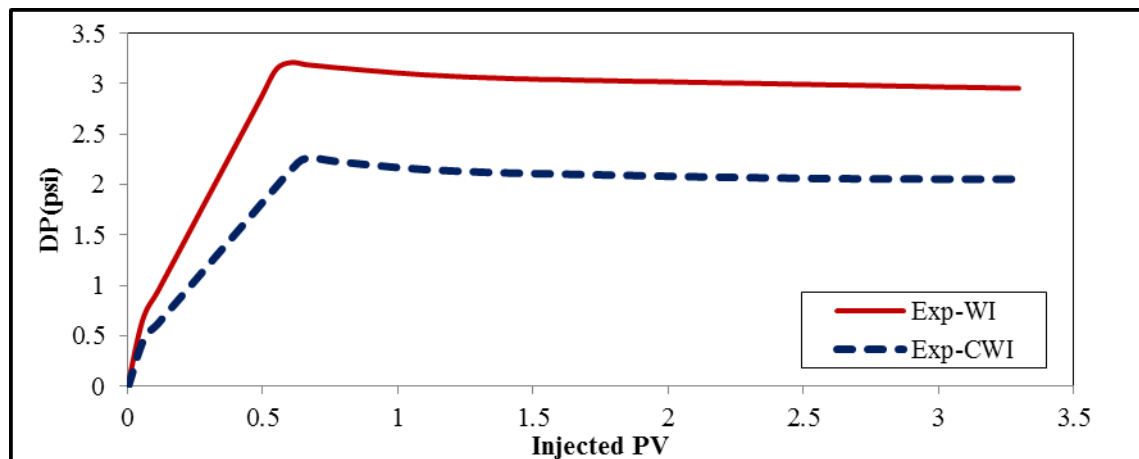


Fig. 2b: Comparison of DP data of the WI and CWI experiments, MW core [5].

#### 211 4. Results and Discussions

212 In our previous paper, for the WW core, the WI experiment was simulated first using our  
213 developed simulator. The water-oil relative permeability ( $K_r$ ) and capillary pressure ( $P_c$ )  
214 based on Corey correlations was obtained through history matching of the WI core

215 production data applying our GA-based optimization program. Next the CWI experiment was  
 216 simulated using Kr and Pc from the WI experiment (WI-Kr and WI-Pc). The unknown MTC  
 217 parameter was obtained by history matching of the CWI production data. The optimal value  
 218 obtained for MTC was 5E-7 (1/sec). It was discussed and shown that oil swelling was the  
 219 main mechanism leading to additional oil recovery of CWI over WI in that experiment. An  
 220 oil swelling factor of 15% was estimated. A similar procedure was followed here to simulate  
 221 MW coreflood experiments. Initially the WI experiment was history matched using GA  
 222 program to obtain Corey-based Kr and Pc curves through a history matching experiment.  
 223 Here, the devolved simulator in its black-oil mode (zero mass transfer and CO<sub>2</sub>  
 224 concentration) was linked to the GA program. The Corey parameters of Kr curves are  $k_{wmax}$ ,  
 225  $n_w$ ,  $K_{omax}$ ,  $n_o$ ,  $S_{or}$  and  $S_{wc}$ . The coreflood experiment had been carried out with zero initial water  
 226 saturation, therefore in the GA program,  $s_{wc}$  was set to zero and  $k_{omax}$  was set to one  
 227 accordingly.  $s_{or}$  was calculated from material balance and core production data to be 0.41.  
 228 The  $k_{wmax}$  was calculated based on the Darcy equation (shown below) to be 0.074.

$$k_{wmax} = \frac{(\frac{q_{inj}}{A}) \times \mu_{water} \times L}{k \times DP_{endpoint}} \quad (1)$$

229 where  $q_{inj}$  is the injection rate, A is the cross section area of the core,  $\mu_w$  is the water  
 230 viscosity, L is the core length, k is the absolute permeability and  $DP_{endp\ int}$  is the endpoint  
 231 value on the DP curve. Therefore, the only unknown parameters were  $n_w$  and  $n_o$  to be  
 232 optimized. The Pc curve was defined based on the Brooks-Corey correlation[25]. However,  
 233 for a mixed-wet system, the capillary pressure curve can also be negative [26-28] which  
 234 cannot be captured by Brooks-Corey correlation. This is because in a mixed-wet rock, some  
 235 pores are water-wet and some pores are oil-wet and if we define  $Pc=P_w-P_o$  for all the pores,  
 236 capillary pressure can also have a negative part. Therefore, Brooks-Corey correlation was  
 237 modified to predict both positive and negative capillary pressures as follows:

$$P_c = p_{ce} \left( \frac{s_w - s_{wc}}{1 - s_{wc} - s_{or}} \right)^{-\frac{1}{\lambda}} - P_{cmax}/\beta \quad (2)$$

238

239 where  $p_{ce}$  is the entry capillary pressure (atm),  $\lambda$  is the pore-size distribution index.  $P_{cmax}$   
 240 is the maximum  $P_c$  (i.e.  $P_c$  at connate water saturation) and  $\beta$  is an unknown parameter. In  
 241 the above equation, the positive term of  $P_{cmax}/\beta$  shows a fraction of maximum  $P_c$  subtracted  
 242 from the main Brooks-Corey correlation to also have a negative  $P_c$ . Similar modification has  
 243 been suggested in the literature[28].  $p_{ce}$ ,  $\lambda$  and  $\beta$  parameters together with  $n_w$  and  $n_o$  were  
 244 determined by the GA program. Table 2 shows the initial uncertainty range of each parameter  
 245 used by the GA during the optimization experiment. These data were selected to be consistent  
 246 with typical Corey and Brooks-Corey parameters obtained for real oil reservoirs [23].

247

248

Table 2: Initial uncertainty range of parameters used in GA.

Kr and Pc parameters	$n_w$	$n_o$	$p_{ce}$ (atm)	$\lambda$	$\beta$
initial uncertainty range	1-5	1-5	0-15	0.2-10	1-25

249

250 The misfit (objective function) to be minimised was defined based on summation of  
 251 absolute relative errors of TOP and DP data ('n' data points) as follows:

$$\text{Misfit} = \sum_{i=1}^n \left| \frac{DP_{\text{real}} - DP_{\text{predicted}}}{DP_{\text{real}}} \right|_i + \sum_{i=1}^n \left| \frac{TOP_{\text{real}} - TOP_{\text{predicted}}}{TOP_{\text{real}}} \right|_i \quad (3)$$

252 A minimum misfit of 0.78 has been obtained at the end of the optimisation. The optimal  
 253 values of the Kr and Pc parameters obtained are summarized in Table 3.

254

255

Table 3: The optimal values of the Kr and Pc parameters, WI experiment.

Parameters	$n_w$	$n_o$	$s_{wc}$	$p_{ce}$ (atm)	$\frac{1}{\lambda}$	$\beta$
Optimal values	2.5	2 .25	0	0.02	0 .22	17

256

257 Figs. 3 and 4 shows Kr and Pc curves respectively based on the data mentioned above. It is  
 258 worth mentioning that based on the obtained capillary pressure curve which is positive,  
 259 perhaps the contribution of water-wet pores has been more dominant. However, another  
 260 possibility is that after the aging process, the core has changed to be intermediate-wet rather  
 261 than the mixed-wet and therefore the intermediate wettability might be a more correct term  
 262 for this core. It can be noted that the capillary pressure is small as the core is homogeneous,  
 263 with high permeability. Figs. 5a and 5b show the history matched experimental TOP and DP  
 264 data, respectively.

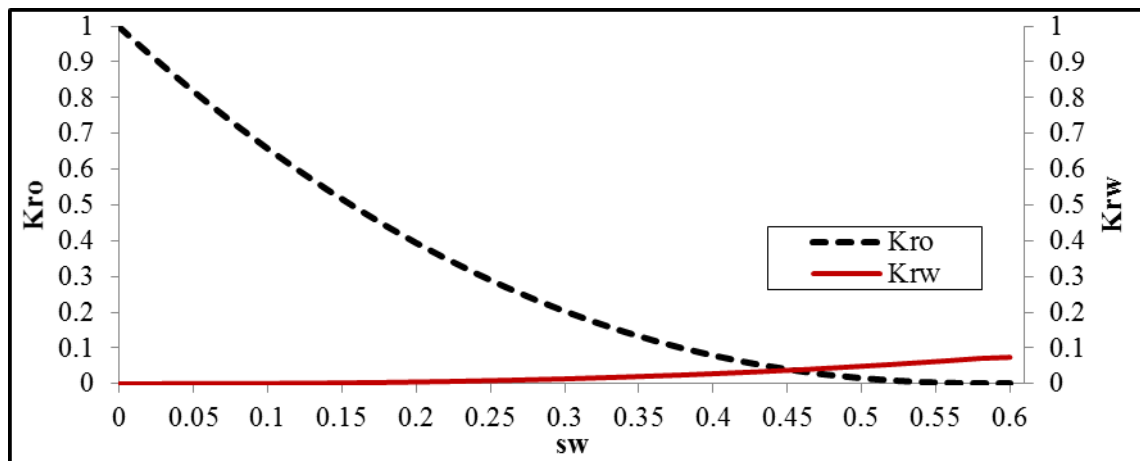


Fig. 3: Optimized  $K_{r_{w-o}}$  curve, WI test.

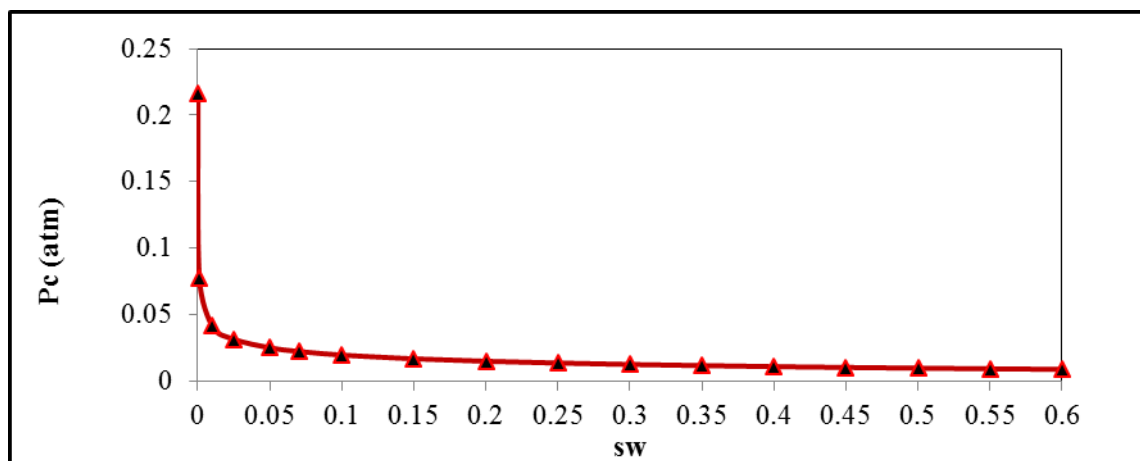


Fig. 4: Optimized Pc curve, WI test.

265  
266  
267

268  
269  
270



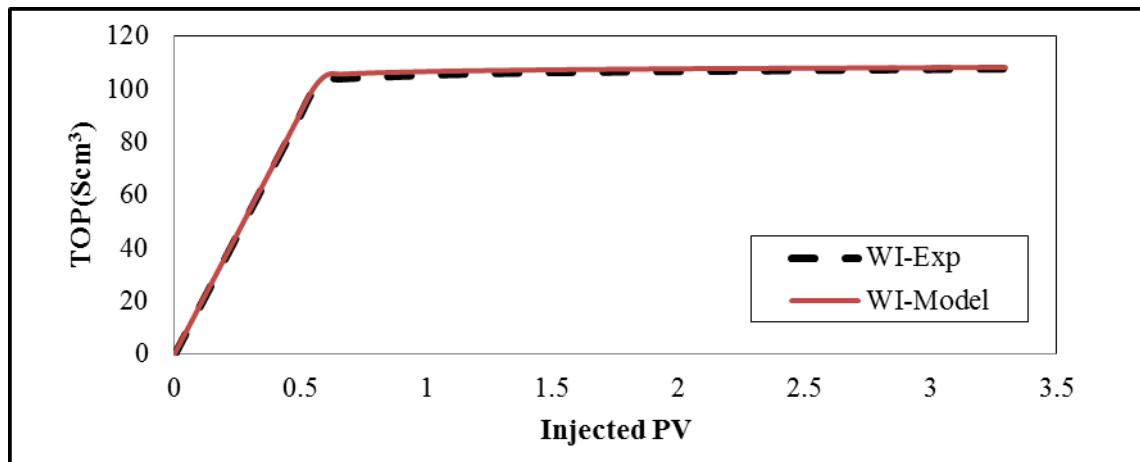


Fig. 5a: History matched TOP-WI data by the developed simulator (model).

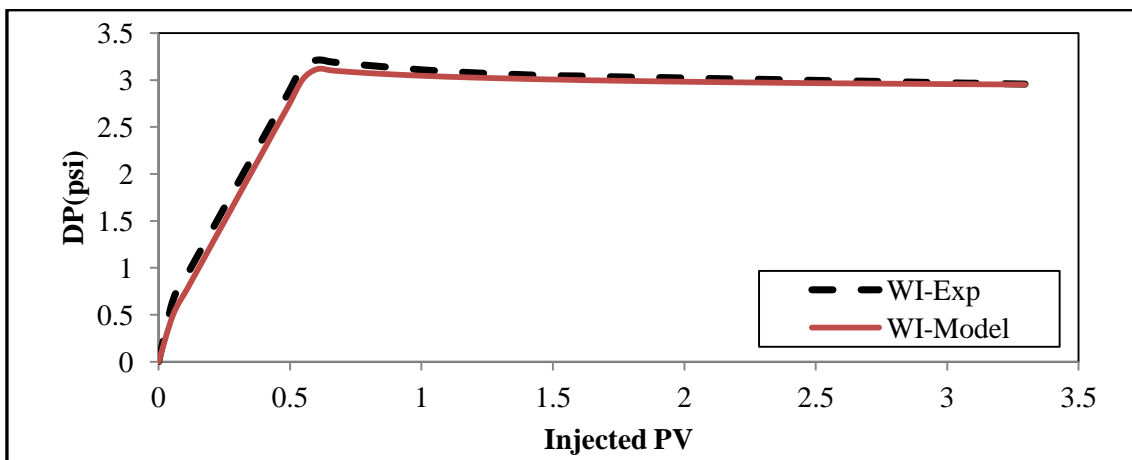


Fig. 5b: History matched DP-WI data by the developed simulator (model).

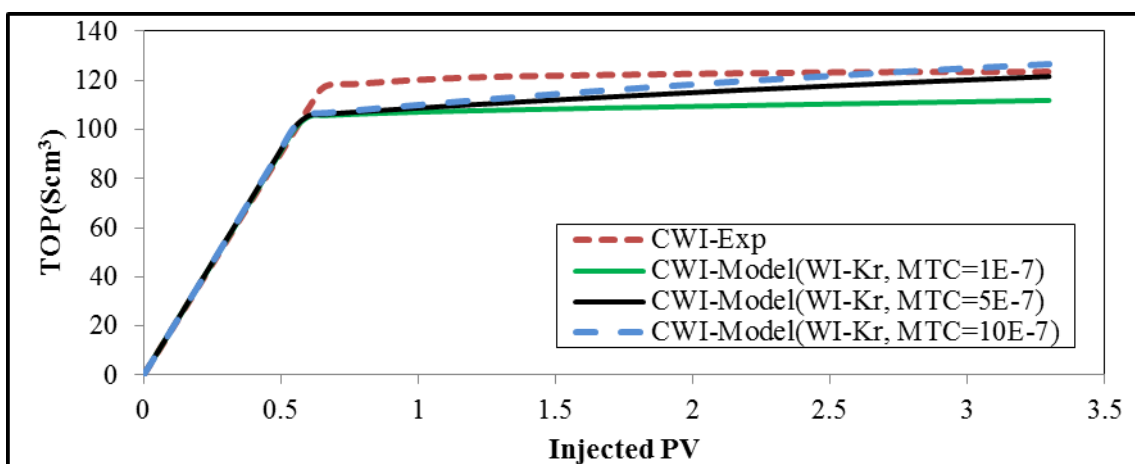
271  
272  
273

274  
275  
276

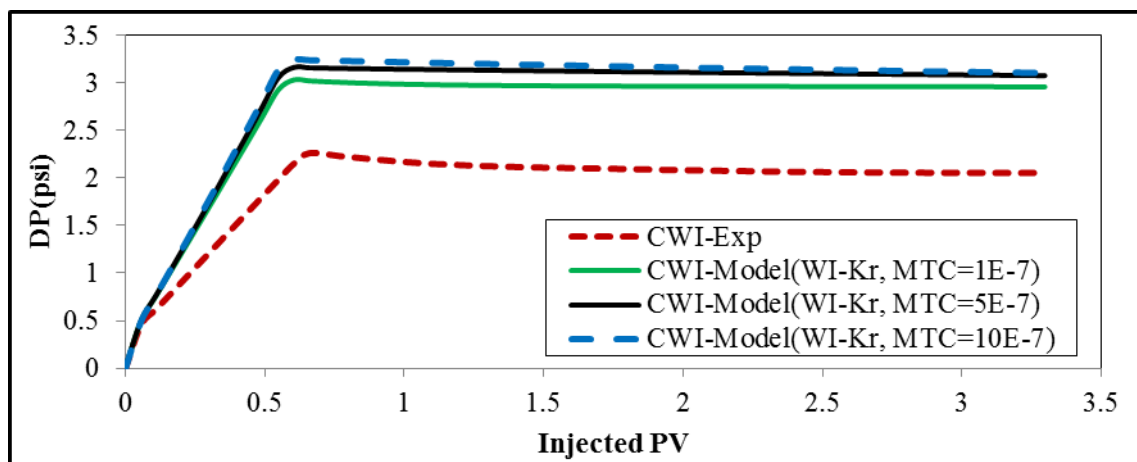
277 It is worth mentioning that it was assumed the flow is stable. That is, it was assumed that  
 278 there is no instability in flow and the discrepancy in flow behavior of water-wet and mixed-  
 279 wet cores reflected in production curves specifically at breakthrough point is not due to  
 280 instability in flow i.e. is not due to for example viscous fingering. This is because, the  
 281 viscosity of water and decane fluids used during test are small and very similar and the core  
 282 was homogenous. It should be noted that the number of gridblocks in our simulations was  
 283 optimized to be 200 when further refining of grids did not change the results predicted by the  
 284 simulator. Moreover, each simulation run took around two minutes to be completed.

285 Next the simulation of CWI was carried out using the developed simulator in its  
 286 compositional mode. Initially the MTC and relative permeability curves were unknown.  
 287 Similar to that for water-wet core, here, first the WI-Kr was used and it was tried to only tune

288 the MTC value and match the core production data. Figs. 6a and 6b demonstrate the effect of  
 289 MTC value on TOP and DP data respectively, predicted by the developed simulator (model).  
 290 Figs. 6a and 6b show that increasing MTC values leads to an increase in the TOP data with  
 291 minimal effect on DP data while, compared to the WI process, the DP values of the CWI  
 292 have reduced during the test. Additionally, Fig. 6a shows that the MTC only affects the oil  
 293 production after breakthrough point and hence the TOP cannot be fully matched if MTC is  
 294 used as the only unknown parameter of the history matching process to be tuned.



295 Fig. 6a: Effect of MTC on TOP-CWI data predicted by the model using WI-Kr.  
 296



297 Fig. 6b: Effect of MTC on DP-CWI data predicted by the model using WI-Kr.  
 298  
 299

300 Therefore, it was concluded that when using the water-oil relative permeability from the  
 301 WI experiment, it is not possible to match the CWI experimental data by only tuning the  
 302 MTC. In other words, both the MTC and relative permeability are needed to be tuned so that  
 303 the model can predict the experimental data of CWI appropriately. That is, the role and

304 contribution of the mass transfer term in the equations is such that it cannot capture the all  
305 mechanisms happening during the CWI process. The mass transfer term contributes mainly  
306 towards the oil swelling as it adds some mass to the oil phase, which, in turn, increases the oil  
307 volume, resulting in the swelling of the oil. It should be noted that, the viscosity of normal  
308 decane is very small (around 0.8cp) and therefore, as discussed in our previous paper, it is not  
309 expected that the viscosity reduction to be an important mechanism (viscosity of decane can  
310 reduce to around 0.3cp, if it is fully saturated with CO<sub>2</sub>). Moreover, as discussed in our  
311 previous paper, the level of IFT change between carbonated water and decane fluids is not  
312 high making the IFT reduction a negligible recovery mechanism here. To find about the  
313 additional mechanisms contributing during CWI, it is worth comparing the TOP and DP data  
314 of CWI and WI tests (Figs. 1b and 2b). It can be noted that, the breakthrough point is shifted  
315 to the right showing a delayed breakthrough time during CWI and also the DP values have  
316 reduced. This may be due to invasion of the carbonated water into the oil-wet pores which are  
317 occupied by the oil. The surfaces of these pores are wetted by the oil components and a layer  
318 of oil film has adhered to the wall. Carbonated water could probably extract and wash away  
319 some part of this oil, i.e. the oil layer which is adhered to the surface of the pores and thus has  
320 led to a reduction of residual oil. This has resulted in more oil recovery with a delayed  
321 breakthrough time, and also a reduction in the DP values. If this possible process happens, the  
322 DP values decreases as there is a larger area available for the water to pass through the pores  
323 (i.e. water mobility improvement). This mechanism, which is not seen in the water-wet core,  
324 can be related to the wettability modification (or alteration) of the rock surface, which allows  
325 the oil layer to be separated from the surface of the pores and be produced during the CWI  
326 process. Wettability alteration by CWI has been reported in the literature as mentioned  
327 before. To incorporate this into the simulation, the Kr curve from the WI experiment should

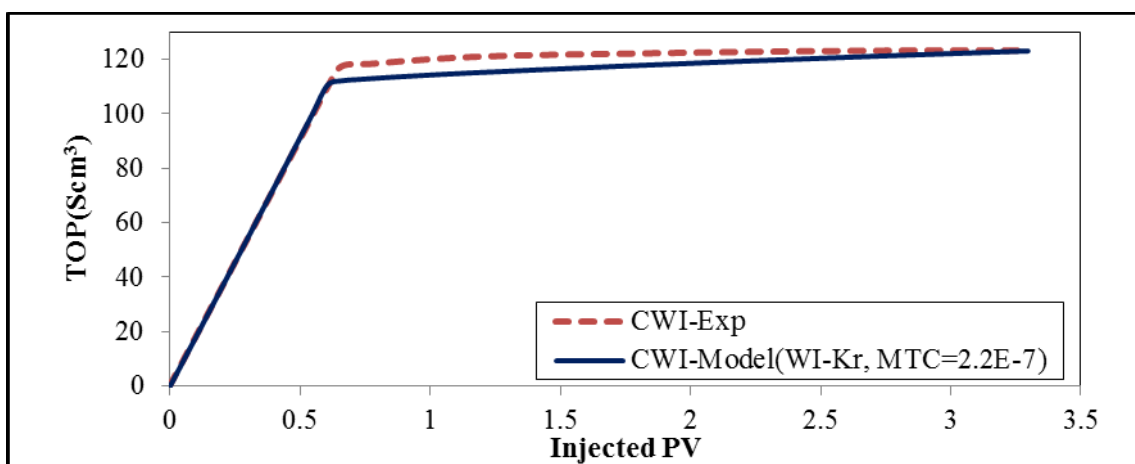
328 be modified to capture the effect of wettability alteration during CWI experiment. That is, for  
329 the MW, the Kr curve for the CWI test is not the same as that for the WI experiment.

330 It is important to exclude the oil swelling in the Kr curve in the model as it is going to be  
331 reflected in the mass transfer term (MTC parameter). Therefore, the main concern and aim at  
332 this stage is to quantify and differentiate the role of the oil swelling mechanism and  
333 wettability alteration in the CWI performance. It should be noted that, it is difficult to  
334 estimate the oil swelling in this MW coreflood experiment explicitly, as wettability is also  
335 changed in this system. Therefore, to quantify the oil swelling here, the WW core data were  
336 used here.

337 It was first assumed that the same oil swelling and accordingly the same MTC value as  
338 that estimated for the WW core is also valid for the MW coreflood test (i.e. 15% swelling and  
339  $MTC=5E-7$  1/sec). However, Figs. 6a and 6b presented above, shows that only the endpoint  
340 of the TOP data is matched using this MTC. It had been shown before that for the WW  
341 core[1], the oil swelling mainly contributes to additional oil recovery after the breakthrough  
342 point and is inherently captured through MTC parameter in the model. In the MW coreflood  
343 experiment, as shown in Fig. 1a and discussed above, 9% additional oil recovery was  
344 obtained by CWI at end of the experiment after the breakthrough point. However, in the MW  
345 core, the additional oil recovery was 4% (Fig. 1b). Therefore, it seems that the importance of  
346 the oil swelling and the magnitude of the MTC in the MW core is not exactly the same as that  
347 in the WW core. The MTC value for the MW coreflood experiment can be estimated to be  
348  $2.2E-7$  1/sec, using 9% and 4% additional oil recovery obtained over the breakthrough point  
349 during the WW and MW coreflood experiments respectively ( $\frac{4}{9} \times 5E-7 = 2.2E-7$ ). Moreover, it  
350 should be considered that in the WW coreflood experiment, total pore volume of injected  
351 carbonated water was 4.1 while in the MW coreflood experiment it was 3.3. Therefore, the  
352 amount of mass transferred and resultant oil swelling in the MW coreflood experiment should

353 be lower than that in the WW coreflood experiment (i.e. lower than 15%). The oil swelling  
 354 here can be estimated to be 12%, using 4.1 and 3.3 total injected PV during WW and MW  
 355 coreflood experiments respectively ( $\frac{3.3}{4.1} \times 15\% = 12\%$ ). It should be noted that the suggested  
 356 procedure for the estimation of MTC and swelling in this MW core, based on the data of the  
 357 WW core and using the linear relations, is an estimation and it could be verified if more  
 358 experimental data were available. Nevertheless, to support this procedure more, a similar  
 359 MTC has been obtained from a different method as discussed later on.

360 To match the TOP and DP data, first the residual oil saturation is adjusted to capture the  
 361 swelling mechanism. Using the experimental data and based on the material balance, the  
 362 calculated residual oil saturation ( $s_{or}$ ) for WI and CWI tests are 0.41 and 0.32, respectively.  
 363 The 0.32 value is for dead oil saturation, with no CO<sub>2</sub> content and hence, the actual  $s_{or}$  should  
 364 be higher because of its CO<sub>2</sub> content. The estimated oil swelling in this test is 12%.  
 365 Therefore, the swollen residual oil saturation is estimated to be 36% ( $32\% \times 1.12 = 36\%$ ). As  
 366 for the WW core, swollen  $s_{or}$  and not dead  $s_{or}$  needs to be used in the Kr curve and the  
 367 difference should be captured by the MTC parameter. Figs. 7a and 7b show, respectively, the  
 368 TOP and DP data when the  $s_{or}$  in WI-Kr is reduced from 41% to 36% and the MTC is set to  
 369  $2.2E-7$  1/sec.



370  
 371 Fig. 7a: TOP-CWI data from the experiment and from the model when WI-Kr with  $s_{or}=0.36$  was  
 372 used.  
 373

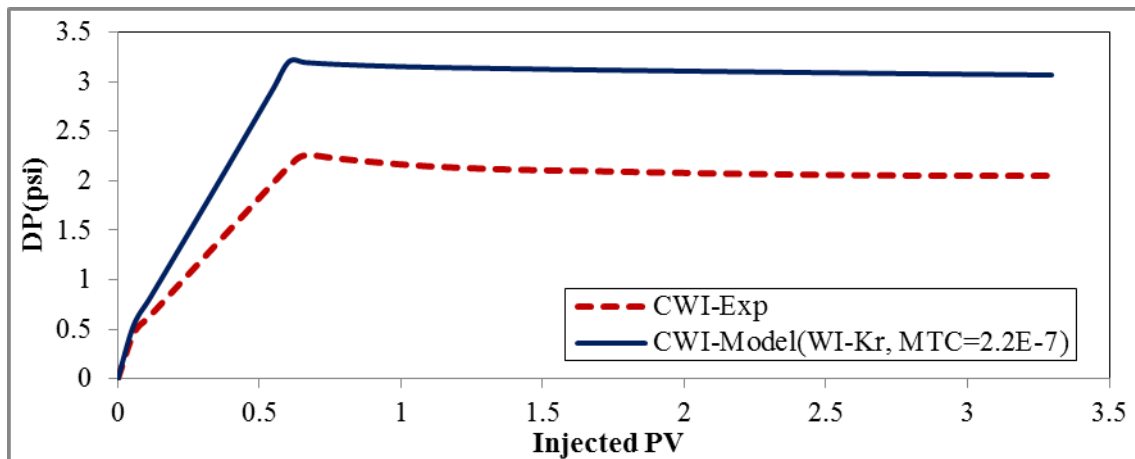
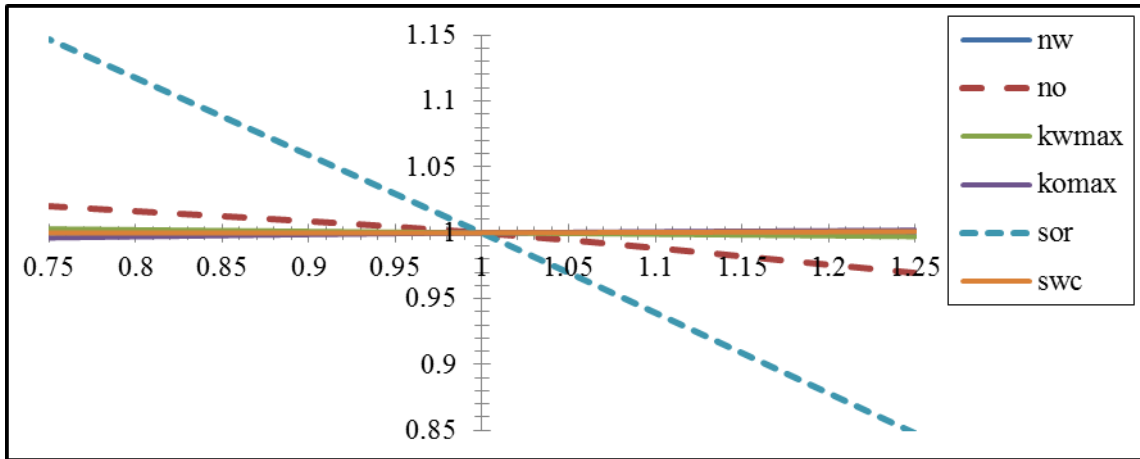


Fig. 7b: DP-CWI data from the experiment and from the model when WI-Kr with  $s_{or}=0.36$  was used.

374  
375  
376  
377

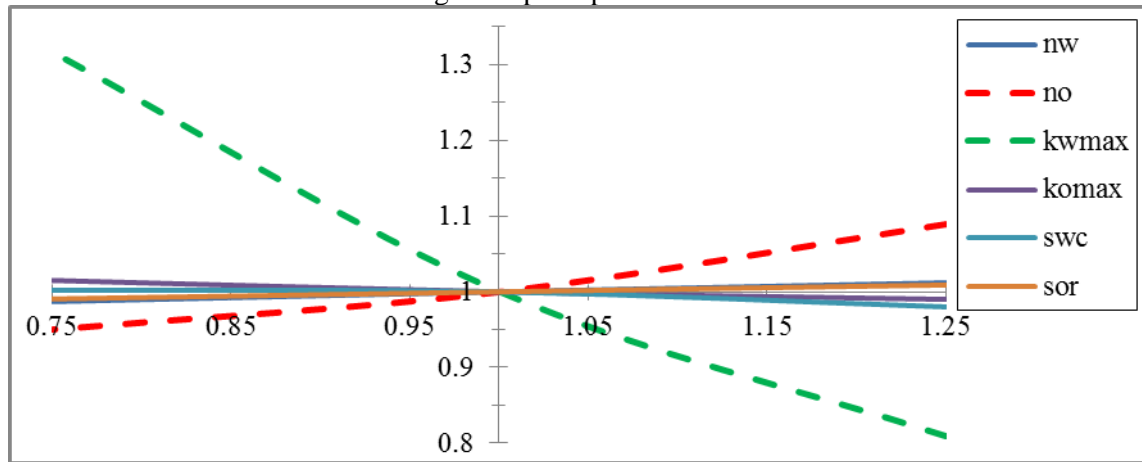
It can be seen that, at this stage, the TOP data is much closer to the experimental values (compared to Fig. 6a), while predicted DP data are still far away from the experimental data. It seems that the rest of data points on TOP and DP curves need to be matched by tuning the relative permeability curve to capture the wettability alteration effect. The Kr curve can be tuned manually as well as automatically using the GA program. To manually tune the Kr curve, a sensitivity analysis on the Corey type relative permeability curve was performed first. Figs. 8a and 8b are the spider plots, which show the impact of Corey relative permeability parameters on the predicted TOP and DP data, respectively. Fig 8a shows for example, if  $s_{or}$  is increased by 25% in the simulator, the predicted TOP decreases by 15%. It can be observed that the TOP data are mainly sensitive to the  $s_{or}$  value, whilst the DP data are sensitive to the  $k_{wmax}$  value. Moreover, the  $n_o$  value affects both TOP and DP data slightly.

378  
379  
380  
381  
382  
383  
384  
385  
386  
387  
388



389  
390

Fig. 8a: Spider plot for TOP.



391  
392  
393

Fig. 8b: Spider plot for DP.

394 Considering the above results, first the TOP data were matched. To do that, the rest of the  
 395 TOP data points were history matched by tuning the  $n_o$  Corey component and after a few  
 396 trials, the  $n_o$  Corey component from the water injection test was reduced by 25% to have  
 397  $n_o=1.7$ . It should be noted that a lower  $n_o$  value means better oil mobility. Later, the DP data  
 398 were history matched manually and, after a few trials,  $k_{wmax}$  from the water injection test was  
 399 increased by 36% to have  $k_{wmax}=0.101$ . It should be noted that a higher value of  $k_{wmax}$  means  
 400 higher water mobility and it only affects the DP data, as shown during the sensitivity analysis  
 401 on the Corey parameters. The misfit value of this manual systematic tuning approach was  
 402 1.42.

403 In the second approach, the GA program was used to estimate the optimal values of MTC,  
 404  $k_{wmax}$ ,  $n_o$  and  $s_{or}$  automatically. It should be noted that in this exercise, the rest of the Corey

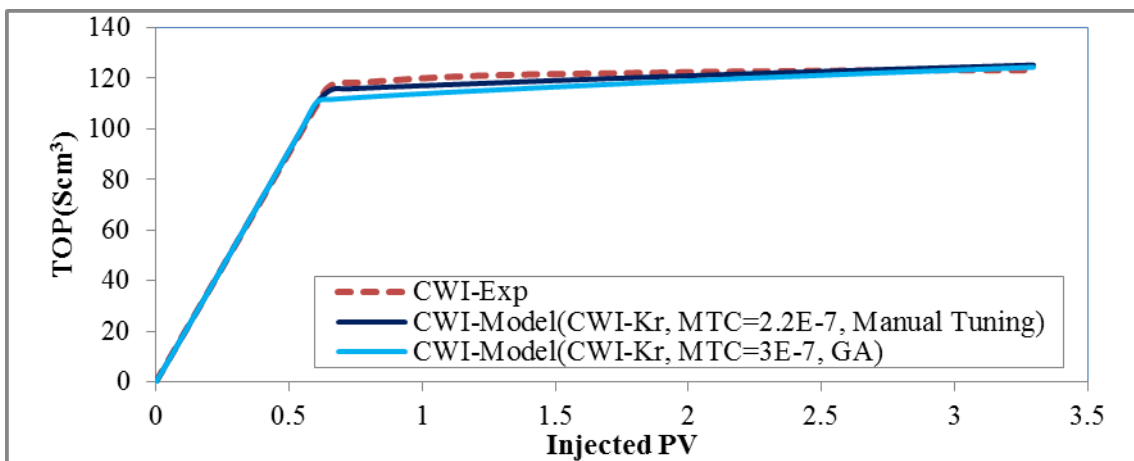
405 parameters were the same as those of the WI test. The minimum misfit value obtained by GA  
 406 was 1.65. Table 4 compares the optimal parameters of CWI-Kr and MTC obtained by manual  
 407 tuning and the GA program.

408 Table 4: Optimal parameters of CWI-Kr and MTC obtained by manual tuning and GA program.

	parameters	$n_w$	$n_o$	$k_{wmax}$	$k_{omax}$	$S_{or}$	$S_{wc}$	MTC
Method	GA	2.5	2.0	0.103	1.0	0.37	0.0	3.0E-7
	Manual tuning	2.5	1.7	0.101	1.0	0.36	0.0	2.2E-7

409

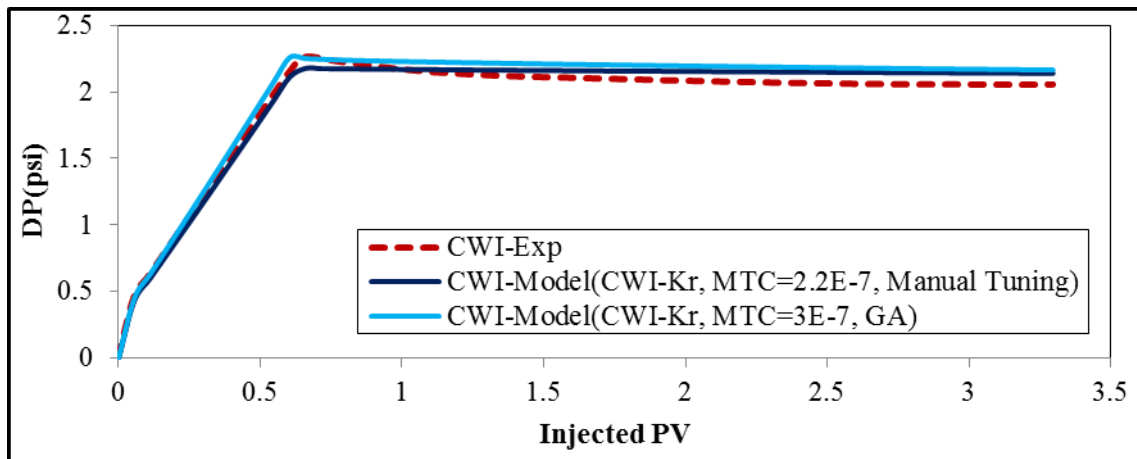
410 It can be seen that the values obtained are almost the same supporting the manual tuning  
 411 procedure suggested above for obtaining the Kr curve. Moreover, this can verify the  
 412 procedure suggested above to estimate the MTC from WW core data. Figs. 9a and 9b  
 413 compare respectively the TOP and DP data from the experiments and those predicted by the  
 414 model using the optimal values of Table 4. It can be seen clearly that the simulator has  
 415 predicted the TOP and DP data properly.



416

417 Fig. 9a: TOP-CWI data from the experiment and from the model when optimal parameters by GA and  
 418 manual tuning (Table 4) was used.





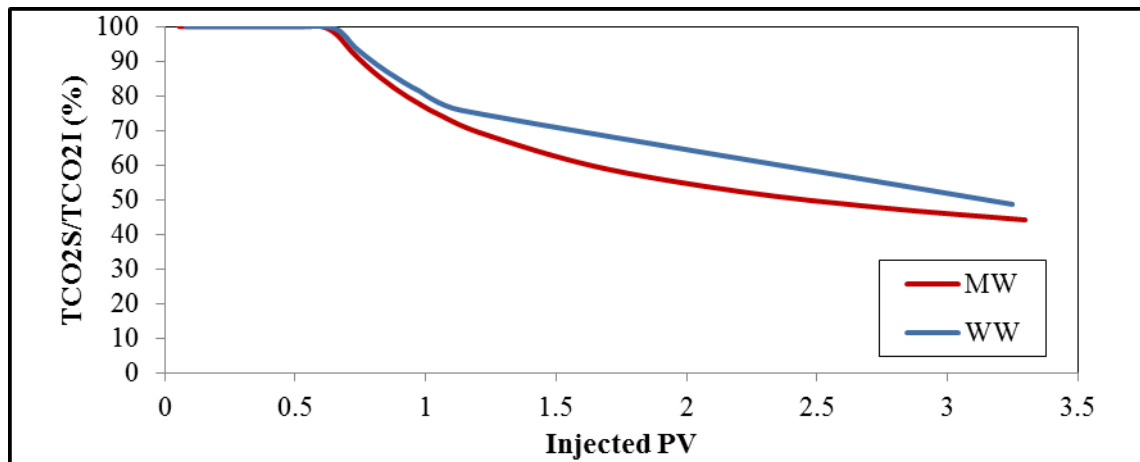
419 Fig. 9b: DP-CWI data from the experiment and from the model when optimal parameters by GA and  
 420 manual tuning (Table 4) was used.  
 421  
 422

423 It should be noted that during automatic history matching four parameters were optimised  
 424 simultaneously while during manual tuning, parameters were tuned separately and step by  
 425 step in a systematic way. This can explain why the misfit value by manual tuning is slightly  
 426 lower than that by the GA.

427 In this paper, the results of a coreflood experiment was investigated and simulated. In  
 428 terms of uncertainty and compared to the real reservoirs, the core properties such as  
 429 permeability and porosity as input data to the model are associated with less uncertainty.  
 430 Here, the reported data measured in the laboratory including core properties and the  
 431 production data have been assumed to be relatively certain. However, if the measurement  
 432 errors are large, it is expected to be difficult to obtain a close and reliable match between  
 433 experimental and predicted results. Moreover, perhaps, the main source of uncertainty in this  
 434 paper are the MTC parameter, Kr curve and Pc curve as these data were obtained through a  
 435 history matching process. That is, through an inversion process, these input parameters were  
 436 calibrated such that the simulator could predict the same production data as those from the  
 437 experiment. Considering the inherent uncertain nature of inversion problems, it is important  
 438 to carefully consider if the answer is unique and reliable. To reduce the uncertainty in this  
 439 work, we followed a systematic approach during history matching including a sensitivity

440 analysis step, manual tuning and GA optimization. In addition, for each experiment, the GA  
441 program was run two times to help with reducing the uncertainty of the inversion problem.  
442 Next, similar to the WW core, ECLIPSE300 (E300) compositional simulator was also used  
443 here to simulate the CWI process and compare its results with them from our model. A  
444 similar E300 model with the same fluid properties and EOS as mentioned in our previous  
445 paper was created here. The optimal CWI-Kr obtained above was also used in the E300.  
446 Similar to the WW core, E300 over predicted the oil recovery factor. We artificially increased  
447 the optimal MTC value obtained above (i.e.  $2.2E-7$  1/sec) in the model by a factor of 5 and  
448 the oil RF predicted by the model increased and became the same as that predicted by E300.  
449 It should be mentioned that, in our model, we are able to adjust the amount of CO<sub>2</sub> transfer  
450 between the phases however in E300 the CO<sub>2</sub> transfer is imposed by equilibrium criterion.

451 In next stage, our simulator was used to study the CO<sub>2</sub> storage in the MW core. Fig. 10  
452 compares the CO<sub>2</sub> storage profile (total CO<sub>2</sub> stored (TCO2S) divided by total CO<sub>2</sub> injected  
453 (TCO2I) versus injected PV of CW) in the WW and MW cores as predicted by the simulator.  
454 It can be seen that after 3.3 PV of CW injected, around 44% of the injected CO<sub>2</sub> has been  
455 stored in the MW core while it is around 49% for the WW core. It should be noted that, the  
456 CO<sub>2</sub> has stored as it is dissolved in the remaining oil and water in the cores at end of the  
457 experiments and as CO<sub>2</sub> solubility in decane is much higher than that in water, CO<sub>2</sub> is mainly  
458 in the oil phase inside the cores. As a result, if more oil can be produced due to wettability  
459 alteration, more CO<sub>2</sub> will be carried out of the core. This is the reason that a sharper decline  
460 can be seen for the MW core in Fig. 10.



461  
 462 Fig. 10: Comparing  $(\frac{TCO2S}{TCO2I} \times 100)$  predicted by the simulator in MW with those in WW from our  
 463 previous paper.  
 464

465 **5. Summary and Conclusions**

466 In this work, the previously developed simulator was used to study CWI in an aged MW  
 467 core. First, experimental data of CWI in the WW and MW cores were compared to gain a  
 468 better understanding of the the main potential mechanisms. It was noted that CWI in the MW  
 469 core had a better performance than that in the WW core. In the WW core, DP-WI and DP-  
 470 CWI data were the same while TOP-CWI data was higher than TOP-WI only after the  
 471 breakthrough point. This higher oil recovery was attributed to the oil swelling by the CO<sub>2</sub>  
 472 component. In the WW, DP-CWI data were lower than DP-WI, which was attributed to the  
 473 wettability wettability alteration. Moreover, the TOP-CWI data were higher than TOP-WI,  
 474 with a shift in breakthrough point. This shift was also attributed to the wettability alteration.  
 475 Furthermore, some oil production after the breakthrough point was observed during CWI  
 476 experiment, which was explained as the effect of oil swelling. Next, WI experiment was  
 477 simulated and history matched when a proper Kr and Pc curve was obtained. To define Pc,  
 478 Brooks-Corey correlation was modified such that a negative Pc value can also be predicted.  
 479 However finally a positive Pc was obtained. Next CWI was simulated when WI-Kr and MTC  
 480 parameter were modified manually and also using GA program to history match the core  
 481 production data. It was observed that opposed to the WW core, for the MW core studied here,

482 Kr curve was not the same for both the WI and CWI processes. It was also attempted to  
483 quantify the swelling effect and wettability alteration in the model systematically. Moreover  
484 CO<sub>2</sub> storage was also considered and it was observed that more CO<sub>2</sub> could be stored in the  
485 WW core compared to that in the MW core.

#### 486 **Nomenclatures**

487  $\omega$  = Mass fraction of the oil component in the oil-CO<sub>2</sub> mixture

488  $\omega^{CO_2}$  = Mass fraction of the CO<sub>2</sub> component in the oil-CO<sub>2</sub> mixture

489  $\omega_w^{CO_2}$  = Mass fraction of the CO<sub>2</sub> component in the water-CO<sub>2</sub> mixture

490  $\omega_w^w$  = Mass fraction of the water component in the water-CO<sub>2</sub> mixture

491  $C^{CO_2}$  = CO<sub>2</sub> concentration in the oil-CO<sub>2</sub> mixture (g/cm<sup>3</sup>)

492  $C_w^{CO_2}$  = CO<sub>2</sub> concentration in the water-CO<sub>2</sub> mixture (g/cm<sup>3</sup>)

493  $C^{CO_2*}$  = CO<sub>2</sub> concentration (g/cm<sup>3</sup>) in oil phase at the equilibrium state

494  $C_w^{CO_2*}$  = CO<sub>2</sub> concentration (g/cm<sup>3</sup>) in water phase at the equilibrium state

495  $k_{eq}$  = Distribution coefficient, here is 9.6 [1].

496 MTC=Pseudo mass transfer coefficient (MTC) (1/sec)

497  $p$ = phase pressure (atm)

498  $s$ =phase saturation

499  $k$ =absolute permeability (mD)

500  $\varphi$ = porosity

501  $\mu$  = Viscosity of the oil-CO<sub>2</sub> mixture at test conditions (cP)

502  $\mu_w$  = Viscosity of the water-CO<sub>2</sub> mixture at test conditions (cP)

503  $\mu_{water}$  = Viscosity of pure water at test conditions (cP)

504  $p_{ce}$  = entry capillary pressure (atm)

505  $\lambda$ = pore-size distribution index

506  $P_{cmax}$  = maximum Pc (i.e. Pc at connate water saturation)

507  $\beta$  = an unknown parameter in Pc correlation.  
508  $K = (k_m \times a)$  with ' $k_m$ ' is the overall mass transfer coefficient (cm/sec) and 'a' is the specific  
509 interfacial area (1/cm).  
510  $N_c$  = capillary number  
511  $u_{df}$  = velocity of displacing fluid, here is carbonated water (m/sec)  
512  $\mu_{df}$  = viscosity of displacing fluid, here is carbonated water (kg/m.sec )  
513  
514  $\sigma$  = carbonated water-decane interfacial tension, here is 20E-3 (N/m) [29]

515

## 516 **Acknowledgments**

517 This work has been carried out as part of CWI joint industry project (JIP) at Heriot-Watt  
518 University. The CWI JIP is equally sponsored by Petrobras, Total, BG Group, Abu Dhabi  
519 Company for Onshore Oil Operations (ADCO), Galp Energia and UK Department of Energy  
520 & Climate Change (DECC) which is gratefully acknowledged.

521

## 522 **References**

- 523 [1] J. Foroozesh, M. Jamiolahmady, M. Sohrabi, Mathematical modeling of carbonated  
524 water injection for EOR and CO<sub>2</sub> storage with a focus on mass transfer kinetics, Fuel,  
525 174 (2016) 325-332.  
526 [2] N.I. Kechut, M. Riazi, M. Sohrabi, M. Jamiolahmady, Tertiary oil recovery and CO<sub>2</sub>  
527 Sequestration by carbonated water injection (CWI), in: SPE International Conference on  
528 CO<sub>2</sub> Capture, Storage, and Utilization (SPE No. 139667), New Orleans, LA 2010.  
529 [3] M. Riazi, M. Sohrabi, M. Jamiolahmady, S. Ireland, Oil recovery improvement using  
530 CO<sub>2</sub>-enriched water injection, in: EUROPEC/EAGE Conference and Exhibition (SPE No.  
531 121170), Amsterdam, The Netherlands 2009.  
532 [4] M. Sohrabi, N.I. Kechut, M. Riazi, M. Jamiolahmady, S. Ireland, G. Robertson, Safe  
533 storage of CO<sub>2</sub> together with improved oil recovery by CO<sub>2</sub>-enriched water injection,  
534 Chemical Engineering Research and Design, 89 (2011) 1865-1872.  
535 [5] M. Sohrabi, N.I. Kechut, M. Riazi, M. Jamiolahmady, S. Ireland, G. Robertson,  
536 Coreflooding studies to investigate the potential of carbonated water injection as an injection  
537 strategy for improved oil recovery and CO<sub>2</sub> storage, Transport in porous media, 91 (2012)  
538 101-121.  
539 [6] N.I. Kechut, M. Jamiolahmady, M. Sohrabi, Numerical simulation of experimental  
540 carbonated water injection (CWI) for improved oil recovery and CO<sub>2</sub> storage, Journal of  
541 Petroleum Science and Engineering, 77 (2011) 111-120.  
542 [7] A.H. Alizadeh, M. Khishvand, M.A. Ioannidis, M. Piri, Multi-scale experimental study of  
543 carbonated water injection: An effective process for mobilization and recovery of trapped oil,  
544 Fuel, 132 (2014) 219–235.

- 545 [8] M.A. Ahmadi, M. Zeinali Hasanvand, S. Shokrollahzadeh Behbahani, A.  
546 Nourmohammad, A. Vahidi, M. Amiri, G. Ahmadi, Effect of operational parameters on the  
547 performance of carbonated water injection: Experimental and numerical modeling study, *The*  
548 *Journal of Supercritical Fluids*, 107 (2016) 542-548.
- 549 [9] A. Fathollahi, B. Rostami, Carbonated water injection: Effects of silica nanoparticles and  
550 operating pressure, *The Canadian Journal of Chemical Engineering*, 93 (2015) 1949–1956.
- 551 [10] Y. Dong, B. Dindoruk, C. Ishizawa, E.J. Lewis, An experimental investigation of  
552 carbonated water flooding, in: *SPE Annual Technical Conference and Exhibition (SPE No.*  
553 *145380)*, Denver, Colorado, USA 2011.
- 554 [11] N. Mosavat, F. Torabi, Performance of secondary carbonated water injection in light oil  
555 systems, *Industrial & Engineering Chemistry Research*, 53 (2013) 1262-1273.
- 556 [12] M. Sohrabi, M. Riazi, M. Jamiolahmady, N.I. Kechut, S. Ireland, G. Robertson,  
557 Carbonated water injection (CWI)-a productive way of using CO<sub>2</sub> for oil recovery and CO<sub>2</sub>  
558 storage, *Energy Procedia*, 4 (2011) 2192-2199.
- 559 [13] M. Riazi, M. Sohrabi, M. Jamiolahmady, Experimental study of pore-scale mechanisms  
560 of carbonated water injection, *Transport in porous media*, 86 (2011) 73-86.
- 561 [14] H. Li, S. Zheng, D. Yang, Enhanced Swelling Effect and Viscosity Reduction of  
562 Solvent(s)/CO<sub>2</sub>/Heavy-Oil Systems, *SPE Journal*, 18 (2013) 695-707.
- 563 [15] D. Yang, Y. Gu, P. ontiwachwuthikul, Wettability Determination of the Crude Oil-  
564 Reservoir Brine-Reservoir Rock System with Dissolution of CO<sub>2</sub> at High Pressures and  
565 Elevated Temperatures, *Energy & Fuels*, 22 (2008) 2362–2371.
- 566 [16] M. Seyyedi, M. Sohrabi, A. Farzaneh, Investigation of Rock Wettability Alteration by  
567 Carbonated Water through Contact Angle Measurements, *Energy & Fuels*, 29 (2015) 5544-  
568 5553.
- 569 [17] M. Seyyedi, M. sohrabi, Enhancing Water Imbibition Rate and Oil Recovery by  
570 Carbonated Water in Carbonate and Sandstone Rocks, *Energy & Fuels*, 30 (2016) 285–293.
- 571 [18] S.M. Al-Mutairi, S.A. Abu-Khamsin, T.M. Okasha, M.E. Hossain, An experimental  
572 investigation of wettability alteration during CO<sub>2</sub> immiscible flooding, *Journal of Petroleum*  
573 *Science and Engineering*, 120 (2014) 73-77.
- 574 [19] N. De Nevers, A calculation method for carbonated water flooding, *Society of Petroleum*  
575 *Engineers Journal*, 4 (1964) 9-20.
- 576 [20] MATLAB Software 2012, Genetic Algorithm Toolbox User's Guide in.
- 577 [21] Y.-B. Chang, B.K. Coats, J.S. Nolen, A compositional model for CO<sub>2</sub> floods including  
578 CO<sub>2</sub> solubility in water, *SPE Reservoir Evaluation & Engineering*, 1 (1998) 155-160
- 579 [22] S. Embid, O. Rivas, Simulation of Miscible Displacement with Interphase Mass Transfer  
580 Resistance, *SPE Advanced Technology Series*, 2 (1994) 161-168.
- 581 [23] T. Ahmed, *Reservoir engineering handbook*, Gulf Professional Publishing 2001.
- 582 [24] J. Geller, J. Hunt, Mass transfer from nonaqueous phase organic liquids in water-  
583 saturated porous media, *Water resources research*, 29 (1993) 833-845.
- 584 [25] R. Brooks, T. Corey, Hydraulic properties of porous media, *Hydraulic Paper No. 3*,  
585 *Colorado State University, Fort Collins, Colorado*, (1964) 1–37.
- 586 [26] W.G. Anderson, Wettability literature survey- Part 4: effects of wettability on capillary  
587 pressure, *Journal of Petroleum Technology* 39 (1987) 1283-1300.
- 588 [27] J.O. Helland, S.M. Skjaeveland, Physically based capillary pressure correlation for  
589 mixed-wet reservoirs from bundle-of-tubes model, *SPE Journal* 11 (2006) 171-180.
- 590 [28] S.A. Bradford, F.J. Leij, Fractional wettability effects on two-and three-fluid capillary  
591 pressure-saturation relations, *Journal of Contaminant Hydrology*, 20 (1995) 89-109.
- 592 [29] A. Georgiadis, G. Maitland, J. P. Martin Trusler, A. Bismarck, Interfacial tension  
593 measurements of the (H<sub>2</sub>O+n-Decane + CO<sub>2</sub>) ternary system at elevated pressures and

594 temperatures, ACS Publications, Journal of Chemical &Engineering Data, 56 (2011), 4900-  
595 4908.  
596